Agricultural and Forest Meteorology 274 (2019) 184–194

Contents lists available at ScienceDirect

Agricultural and Forest Meteorology

journal homepage: www.elsevier.com/locate/agrformet

A data-conditioned stochastic parameterization of temporal plant trait variability in an ecohydrological model and the potential for plasticity

Shaoqing Liu[a,*], Gene-Hua Crystal Ng[a,b]

[a] Department of Earth Sciences, University of Minnesota, Twin Cities, Minneapolis, Minnesota, USA
[b] Saint Anthony Falls Laboratory, University of Minnesota, Twin Cities, Minneapolis, Minnesota, USA

ARTICLE INFO

Keywords:
Plant trait
Data-model integration
Ecohydrological models
Stochastic parameterization
Temporal trait variability

ABSTRACT

Recent studies have begun to incorporate spatially variable plant traits into ecohydrological models, but temporal trait variability remains under-studied. Because of its potential to influence ecosystem function, representing stress-induced temporal trait variability into models should be a research priority. We present a new data-model integration approach to identify temporal variability in plant traits and generate stochastic-in-time model parameterizations. The data-conditioned stochastic parameterization was developed within the CLM 4.5 model utilizing global trait data as prior information and tested for a desert shrubland site. A synthetic experiment demonstrated that the framework successfully uncovered time-varying trait values. Using in-situ ecohydrological observations, we found the specific leaf area (SLA) for a common broadleaf-evergreen-shrub to be temporally dynamic and significantly correlated with seasonal water availability. We constructed a regression model based on the data-conditioned SLA estimates and soil wetness and used it to generate stochastic SLA parameters for a 40-year hindcast simulation. The stochastic-in-time SLA parameters resulted in greater productivity and water use efficiency than a standard static parameter. Our stochastic-in-time method can help evaluate stress-induced trait plasticity that extends our understanding beyond sparse spatial plant trait database and improve our ability to simulate carbon and water fluxes under global change.

1. Introduction

Plant functional traits, including morphological, physiological, and phenological attributes, are key characteristics for linking ecological functions and providing a mechanistic understanding of species response to environmental conditions (van Kleunen and Fischer, 2007). Trait plasticity, which arises from genetic diversity and phenotypic plasticity (Nicotra et al., 2010), can allow plants to modify their morphological and/or physiological traits to increase environmental tolerance, making them capable of surviving over an extensive geographic range. Recent studies indicate that phenotypic plasticity rather than genetic diversity likely plays the crucial role in allowing plants to persist in their environments in both the short- and long-term, as it is the most rapid mechanism of response to environmental drivers (Vitasse et al., 2010). Understanding plant plasticity is crucial for predicting changes in species distribution, community composition, and plant productivity under global change.

Different environmental conditions may impose different selective pressures on plants, driving traits to a certain degree of divergence. The spatial variations in plant leaf traits are well-documented, and they tend to relate to plant functional type and climate (Reich et al., 1997; Wright et al., 2004). An “economic spectrum” has been used to describe ecological trade-offs observed in a global data set of leaf measurements spanning ecological and climatic gradients (Wright et al., 2004). On a much smaller spatial scale, leaf traits can vary as much within a canopy with the light environment as across individual plants (Serbin et al., 2014).

Compared to the spatial variation of plant traits, fewer empirical studies examine the temporal variability of traits, presumably due to the challenges of labor-intensive and non-destructive repeat measurements, and this hinders our understanding about the adaptive process of trait plasticity. However, there is evidence for temporal trait variability over seasonal to inter-annual time scales (Reich et al., 2018; Dawson and Bliss, 1993; Damesin et al., 1998; Damesin and Lelarge, 2003). Nouvellon et al. (2010) found that the stand-average specific leaf area (SLA) (ratio of leaf area to dry mass) varied about 20% within one year in a *Eucalyptus* plantation, with lower values occurring in the dry season. Other studies found a decrease in SLA to be generally associated with slower plant growth, which can enhance water use efficiency during drought events (Villar et al., 2005; Poorter et al., 2009). In

---

* Corresponding author.
E-mail address: sqliu@umn.edu (S. Liu).

https://doi.org/10.1016/j.agrformet.2019.05.005
Received 1 February 2019; Received in revised form 3 May 2019; Accepted 7 May 2019

addition to external environmental forces, leaf development causes traits to vary over time. Using leaf spectroscopy at temperate deciduous forest sites, Yang et al. (2016) showed that leaf traits (leaf mass per area – the inverse of SLA, leaf nitrogen per mass, chlorophyll levels, and carotenoid concentrations) varied significantly through different growth stages over a season. Also looking at seasonal changes, Muraoka et al. (2010) found that the photosynthetic capacity (maximum rate of carboxylation at 25 °C, V_{cmax25}) increased dramatically during leaf expansion in the spring, stabilized in mid-summer, and declined in autumn in a temperate deciduous forest site. Plant traits may also evolve over longer time periods of years to decades. Thermal adaptation occurs when the sensitivity of plant respiration to temperature (Q_{10}) decreases over time (Atkin et al., 2000; Atkin and Tjoelker, 2003). Various Free Air Carbon Dioxide Experiments (FACE) also demonstrated photosynthetic acclimation over multiple years, with maximum carboxylation rate of Rubisco (V_{cmax}) and maximum electron transport rate (J_{max}) altering due to nitrogen and water limitation (Ainsworth and Rogers, 2007) and CO_2 fertilization (Leakey et al., 2009).

Despite observed trait variability over space and time, current models generally use fixed plant functional types (PFTs) that are assigned static trait values. For example, the Community Land Model 4.5 (Oleson et al., 2013) implements constant leaf nitrogen per mass (N_m) and SLA, which determine the V_{cmax25} and plant phenology, without considering possible changes induced by environmental stressors. Because plant functional traits directly control ecological function, failure to capture their true variability will bias predictions of ecological fluxes that play an essential role in global water and carbon cycles.

To start to address this fixed-PFT parameterization problem, some studies explicitly incorporated trait variability at the individual plant level, but these are limited to small regional or even site-level applications (Sato et al., 2007; Uriarte et al., 2009). More generally applicable, regression methods have provided spatial distributions of plant parameters based on relationships found between plant traits and environmental conditions such as climate and soil (Verheijen et al., 2015; Butler et al., 2017). Another regional to global strategy implemented multiple plant trait combinations into dynamic vegetation models and filtered for parameters that allow plant growth under the given environmental conditions (Fisher et al., 2015; Pavlick et al., 2012). Some studies extended available trait observations by using them to derive probabilistic trait ranges for ensemble simulations (Wang et al., 2012; Pappas et al., 2016).

These studies present important advances in representing spatially variable plant traits in models but still suffer from some limitations. First are the uncertainties in the trait databases on which many of these studies rely. The global TRY database (Kattge et al., 2011) brings together an unprecedented volume of ground measurements but is still too sparse to fully cover the globe continuously over time, and the correlations among functional traits and environmental variables are generally too weak to make interpolations (Wright et al., 2005; Ordoñez et al., 2009; Coyle et al., 2014). The second limitation relates to how traits are selected for variable representation in the model. Ad hoc selection of traits may neglect those that exhibit the strongest direct physiological response to environmental conditions under study, and it may fail to include traits that co-vary together with traits that are represented (Kleyer and Minden, 2015). Finally, most trait-based modeling studies capture spatial distributions but assume traits to be temporally constant (Wang et al., 2012; Pavlick et al., 2012; Butler et al., 2017). In the few attempts to represent time-dynamic traits, some have assumed relationships in a global trait database to apply not only over space but also over annual intervals (Verheijen, 2013; Verheijen et al., 2015). Another global study applied an assumed trait relationship to dynamic leaf area index (LAI) data from satellite imagery to generate seasonally variable V_{cmax25} model inputs (Ryu et al., 2011). In specialized cases, intensive site-specific measurements allowed for detailed trait dynamics models based on development stage and nutrient supply (Sands and Landsberg, 2002; Almeida et al., 2004; Fontes et al., 2006; Battaglia et al., 2004; Corbeels et al., 2005).

What is still missing is a generally applicable modeling framework that can help identify under-observed temporal variability in plant functional traits and quantify uncertainties in our growing understanding about trait plasticity and its impact on ecohydrological fluxes. To fill this gap, we propose a data-conditioned stochastic parameterization that leverages global plant trait data and spatiotemporally complete remote sensing imagery to estimate dynamic traits for use in prognostic vegetation simulations. We develop the new stochastic-in-time PFT parameterization within the Community Land Model 4.5 (CLM 4.5) and test the method for a desert shrubland site in the Mojave Desert. With highly dynamic climatic conditions, desert shrublands provide an apt test-bed for demonstrating how our approach can be used to investigate trait plasticity in response to irregular water availability. Previous model implementation at the site by Ng et al. (2015) used standard static parameters that successfully generated time-averaged LAI observations but under-simulated sharp transitions and minimum and maximum conditions, suggesting the possibility for dynamic leaf traits in that environment. The current work introduces a new stochastic vegetation parameterization that we anticipate can serve as a framework for assessing trait plasticity across ecosystems. Spatiotemporally stochastic parameterizations have been previously applied to represent uncertainties due to unknown and unresolved processes in atmospheric (Palmer et al., 2009; Palmer, 2012; Christensen et al., 2015), ocean (Kitsios, 2014), and sea-ice interaction (Juricke et al., 2012) models. Hydrologic models have long employed spatially stochastic hydraulic parameters to represent heterogeneous media (*e.g.*, Dagan, 1986; Gelhar, 1986) and temporally stochastic rainfall forcing to represent climatic dynamics (*e.g.*, Eagleson, 1978; Rodriguez-Iturbe et al., 2001).

This paper consists of two parts. First, we use a synthetic experiment to present our proposed stochastic parameterization method and prove its ability to uncover plant trait temporal variability. The second part demonstrates the utility of the new method; we condition ensemble model parameters and simulations on in-situ soil moisture and remotely sensed vegetation data to test the hypothesis that seasonal to interannual moisture conditions drive changes in leaf traits and impact ecohydrological fluxes in desert shrublands.

2. Materials and method

2.1. Study site

Our study site “Kelmet” (elevation: 860 m.a.s.l.) is located in Kelso Valley in the Mojave National Preserve, southeastern California, USA (Fig. 1). Earlier studies in Kelso Valley examined the surficial geology (Miller et al., 2009), soil hydraulic properties (Nimmo et al., 2009; Mirus et al., 2009), and distribution of shrubs (Bedford et al., 2009; Schwinning et al., 2011). Ng et al. (2015) synthesized data from those studies in a static-parameter ecohydrological model to evaluate the relationship among precipitation events, soil moisture, and LAI at a low elevation study area within the valley. The current modeling work uses climate and soil data detailed in Ng et al. (2014, 2015). A brief summary of the site and data is provided here.

A 50-year meteorological time series (1961–2010) shows hot summers with mean July temperature above 35 °C and colder winters with mean December temperature of 5 °C. Mean annual precipitation is 103 mm, with winter rains providing most of the precipitation, and summer convective storms occasionally supplying additional inputs. The dominant vegetation type *Larrea tridentata*, a broadleaf evergreen shrub, covers about 15% of the ground, and co-dominant *Ambrosia dumosa*, a drought-deciduous shrub, covers about 5%; the remainder is mostly bare ground. *Larrea tridentata* (creosote bush) is widely found throughout the Mojave, Sonoran, and Chihuahuan Deserts (Chew and Chew, 1965; Barbour, 1969; Rundel and Gibson, 2005). The site consists of coarse early Holocene soils overlying a deep (≫100 m) water

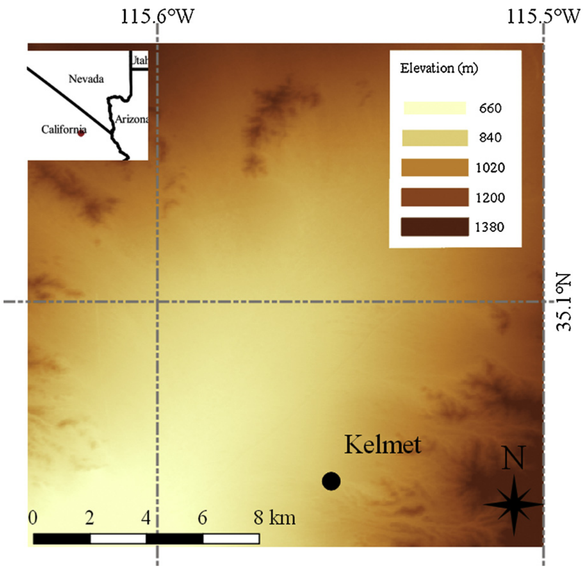

Fig. 1. Study area in the Mojave National Preserve (MNP) in southeastern California, USA (adapted from Ng et al., 2014). The "Kelmet" study site provides the basis for the data assimilation formulation presented here.

table. Soil moisture at 15 and 35 cm soil depths was measured from 2 July 2007 to 31 December 2010. 1-km, 8-day resolution LAI data from MODIS compiled over that period matched well with field-based validation measurements.

2.2. CLM 4.5

This study uses the Community Land Model version 4.5 (CLM4.5), which is the land module of Community Earth System Model 1.2 developed by the National Center for Atmospheric Research (NCAR) (Oleson et al., 2013). CLM4.5 encompasses a comprehensive suite of land-surface processes, mostly using mechanistic parameterizations. With its fully coupled carbon and nitrogen module, ecosystem productivity drives prognostic leaf area and vegetation and soil carbon pools, and nitrogen availability constrains carbon fluxes. The hydrological processes include canopy interception, precipitation throughfall, snow accumulation, sublimation and melt, surface runoff, evapotranspiration, water infiltration and redistribution in soil, and subsurface drainage.

Following Ng et al. (2014), we modified the plant maintenance respiration scheme by applying a multiplicative factor, based on temperature and plant water potential, to respiration using the formulation by Shen et al. (2008) (details in the section S1 of Supplementary Information). This better represents observed shrub respiration acclimation behavior in deserts (Strain and Chase, 1966).

2.3. Data-conditioned stochastic parameterization

Motivated by observed plant trait plasticity, we present a stochastic representation of vegetation parameters, which to our knowledge has not been implemented before in process-based ecohydrological models. Specifically, we apply stochastic perturbations to plant parameters in order to represent unresolved trait dynamics, which are mostly unknown due to a general lack of temporal trait observations. To then address the large uncertainties, we assume that temporal observations of related ecohydrological states are informative about traits and can be used to constrain their dynamics. We thus utilize data-model integration, or data assimilation, to condition stochastically perturbed plant parameters on observations of LAI and soil moisture. The results are estimates of temporally variable plant traits that can be used to evaluate the relationship between trait variability and environmental stressors.

Our data assimilation framework employs the ensemble Kalman Filter (EnKF) (Evensen, 1994) with an augmented state formulation that allows for model parameters to be estimated along with model states (Evensen, 2009). The EnKF provides a Monte Carlo approximation to the traditional Kalman filter using multiple model simulations to estimate an ensemble forecast of model vectors (X_t^f), of which the ensemble covariance represents the forecast error covariance (P^f). Following this forecast step, an analysis (also called "update") step improves the forecast estimate by calculating an updated ensemble of model vectors (X_t^a) based on observations (y_t) at time step t, which are assumed to have an observation covariance of R. X_t^f and X_t^a are both augmented model state vectors that comprise model states (S) and parameters (p). One assimilation cycle is composed of one forecast step and one analysis step. The analysis result at time t serves as the initial condition for the forecast step of the subsequent assimilation cycle at time $t + 1$; assimilation cycles repeat until the final time of the observational period ($t = T$).

Here we use the Ensemble Square Root Filter (EnSRF), an EnKF variant proposed by Whitaker and Hamill (2002) that is less prone to sampling errors than the original EnKF formulation. With EnSRF, the ensemble model mean vector (denoted by an overbar) and the ensemble model deviations from the mean (denoted with prime) are separately updated using Eqs. (1) and (2), respectively:

$$\overline{X}_t^a = \overline{X}_t^f + K(y_t - H\overline{X}_t^f) \tag{1}$$

$$X_t'^a = X_t'^f + M(-HX'^f), \tag{2}$$

where H is the observation operator that converts model states to the observation space, K is the Kalman gain, and M is a transformation matrix. The Kalman gain is calculated by

$$K = P_t^f H^T (HP_t^f H^T + R)^{-1} \tag{3}$$

for the ensemble mean update (Eq. (1)), and the transformation matrix is calculated by

$$M = P_t^f H^T [(\sqrt{HP_t^f H^T + R})^{-1}]^T \times [\sqrt{(HP_t^f H^T + R)} + \sqrt{R}]^{-1} \tag{4}$$

for the perturbation update (Eq. (2)). The final component of the update step is to assemble the ensemble matrix of full model vectors from the mean and perturbations:

$$X_t^a = \overline{X}_t^a \mathbf{1} + X_t'^a \tag{5}$$

where **1** represents a 1xN vector of 1 values, with N as the ensemble size.

Eight vegetation-related parameters in CLM 4.5 are selected for estimation based on a sensitivity study with E3SM (Ricciuto et al., 2017), a land-surface model based on CLM 4.5 (Table 1). Default CLM 4.5 PFT values were used for all remaining plant parameters. EnKF requires parameter values and uncertainty distributions prior to the first analysis step (for $X_{t=0}^f$ and $P_{t=0}^f$). For three of the trait parameters –

Table 1
CLM 4.5 plant parameters included in estimation. "TRY" indicates that the prior information was derived from the TRY database. For other parameters, prior uniform distributions are used with the indicated limits taken from White et al. (2000).

Parameter	Description	Prior
mp_pft	Slope for stomatal conductance-to-photosynthesis in Ball-Berry Model	(5, 12)
rootb_par	Root distribution parameter	TRY
leafcn	The ratio of carbon to nitrogen in leaf	TRY
slatop	SLA at top of canopy	TRY
frootcn	The ratio of carbon to nitrogen in fine root	(35,50)
froot_leaf	Allocation of new fine root C per new leaf C	(0.5,1.5)
flnr	Fraction of leaf N that is in RuBisCO enzyme	(0.01,0.07)
leaf_long	Leaf longevity in years	(0.6,1.5)

SLA, the ratio of carbon to nitrogen in leaves (leafcn), and leaf longevity – we use lognormal distributions based on the global TRY database (Kattge et al., 2011) for the prior uncertainty. The other five parameters do not correspond to commonly measured traits in TRY and are assigned uniform distributions over the range of parameter values reported in White et al. (2000). The EnKF implementation then uses two types of calibration data (y) for the analysis step, MODIS (LAI) and in-situ soil moisture at 15 cm and 35 cm depth. This implementation leverages global vegetation datasets; future work will evaluate the use of satellite soil moisture products instead of in situ measurements.

In a typical EnKF implementation for static parameters, parameters remain constant over the EnKF forecast step, while only model states evolve through Monte Carlo simulations. During each analysis step, parameter estimates in the augmented state do change; however, the end time result usually serves as the final calibrated static model parameter. Our formulation differs by building on the strategy by Hansen and Penland (2007) to use the time series of EnKF analysis results for estimating stochastic properties of parameters. First, we pose a prior stochastic parameterization using a stationary Gaussian first-order autoregressive (AR-1) model, which is incorporated into the EnKF forecast step:

$$p^{t+1} = \alpha^* p^t + \varepsilon \tag{6}$$

$$\varepsilon \sim N(0, h^2 V) \tag{7}$$

$$h = \sqrt{1 - a^2} \tag{8}$$

p^t and p^{t+1} are parameters representing plant traits at the beginning and end of the forecast step, respectively, and α is the first-order autoregressive correlation coefficient (α is set as 0.999). The uncertainty term ε has a variance determined by the smoothing factor (h) and variance value (V). The variance value (V) is adjusted to give the assimilation result with the most favorable statistics in the EnKF implementation. Eqs. (6–8) do not attempt to represent actual mechanistic processes, but they serve as an approximate Markov chain process for generating plausible biophysical dynamics to be further conditioned based on observations. Moradkhani et al. (2005) proposed an EnKF-based parameter estimation approach that similarly evolves parameter values over the forecast step, but that was included as artificial dynamics solely for EnKF performance purposes, while true dynamics motivate our formulation.

We carry out EnKF, employing Eqs. (6–8) for the eight uncertain plant parameters along with CLM 4.5 state simulations for the forecast, such that the parameters now change over both the forecast and analysis steps. Note that in the model state forecast, we assume that the parameters are the major source of uncertainty, and thus we do not include additional model errors. Based on preliminary EnKF tests, an ensemble size of 100 is chosen as a balance of performance and computational feasibility. We found best results by implementing a two-tiered iterative EnKF approach (Fig. 2). Previous studies have applied different iterative extensions of the EnKF that cycle multiple times over periods ranging from a single assimilation cycle to the entire assimilation period in order to further reduce errors and address parameter and state estimate incompatibilities (Moradkhani et al., 2005; Gu and Oliver, 2007; Hendricks Franssen and Kinzelbach, 2008; Ng et al., 2014). Here, we apply two passes of the EnKF over the entire assimilation period, in which a standard static parameter EnKF is first implemented for a first-order approximation of the parameter estimates. The second pass then employs the stochastic formulation (including Eqs. (6–8)) to further constrain temporal variations in the parameters. In the second pass, additional iterations over each assimilation cycle, with separate parameter and state update steps (Sakov et al., 2012), were necessary to generate sufficiently dynamic plant parameters to simulate observed LAI variability. More information about the implementation of stochastic parameterization can be found in the Supplementary Information (Section S2).

After the variance of the parameter estimate stabilizes in the second-pass, the entire time series of ensemble parameter estimates is taken as the final estimate in our formulation. Generating simulations outside the assimilation time period requires identifying relationships in this data-conditioned parameter time series. We identify trait plasticity occurring in response to environmental drivers by searching for correlations between the conditioned parameter time series and environmental factors. These can lead to regression-based models of stochastic plant trait response to stressors, which allows probabilistic predictions of trait plasticity and resulting impacts on carbon and water balances.

2.4. Synthetic experiment setup

We first conduct a synthetic experiment to test if the proposed data-conditioned stochastic parameterization method can constrain environmentally induced plant trait plasticity. Prompted by studies identifying spatiotemporal variability in SLA related to environmental conditions (Misson et al., 2006; Poorter et al., 2009; Nouvellon et al., 2010), we design our experiment around the hypothesis that SLA changes temporally with water stress in desert shrublands. A focus on SLA is also motivated by its strong physiological control on leaf growth (Villar et al., 2005; Wright et al., 2001), which in models is expressed in part as dynamic LAI, the major scaling factor for determining grid cell-level carbon and water fluxes (Olesen et al., 2013). Using the following model, we construct a synthetic true SLA for the broadleaf-evergreen-shrub PFT that is close to the CLM 4.5 default value (0.015 $\text{m}^2\,\text{g}^{-1}$ C) but varies over time based on the soil wetness factor (β):

$$SLA(\text{t}) = 0.010 + 0.005^*\bar{\beta}. \tag{9}$$

The wetness factor in CLM 4.5 ranges from one when the root zone soil is wet to near zero when the root zone soil is dry, and it depends on the root distribution and plant-dependent response properties to soil water stress. The overbar signifies the 30-day average, which was chosen to reflect conditions on a seasonal timescale. Leaf traits are driven by internal constraints of the leaf and whole plant (Westoby et al., 2002), which likely require longer monthly to seasonal time scales to respond to climate fluctuations than photosynthetic capacity traits, which can respond almost immediately to changes in temperature, light, water vapor deficit, and CO_2.

Synthetic LAI and soil moisture observations were generated by implementing the synthetic true SLA time series in CLM with the Kelmet climate and soil inputs and adding random observational noise. These synthetic observations were then used in the stochastic EnKF parameterization formulation (including Eqs. (1–8)), as well as in a standard EnKF implementation for static parameters (in which Eqs. (6–8) are omitted, and the end-time estimate serves as the final calibration result), in order to compare the utility of the new stochastic formulation. To simplify the model implementation in the synthetic experiment, we only include one PFT, broadleaf-evergreen-shrub, to represent the dominant *Larrea tridentata* shrub and only estimate the SLA parameter.

Results for the two synthetic EnKF implementations are evaluated using a scaled mean square error (scMSE), similar to Ng et al. (2014). MSE is determined by:

$$MSE(\text{t}) = \frac{1}{\text{b}} \sum_{\text{j}=1}^{\text{b}} (\bar{\xi}^{\text{j}}(\text{t}) - \xi^{\text{j}}_{tr}(\text{t}))^2 \tag{10}$$

where $\xi^j(t)$ represents the model parameter or state at time step *t*, the overbar signifies the ensemble mean, *tr* signifies the synthetic true value, and *b* denotes the numbers of parameters or states assessed. For parameters, scMSE is calculated by first normalizing each parameter by its prior distribution standard deviation; for model states, scMSE is determined by first normalizing each state by the synthetic true mean value over time:

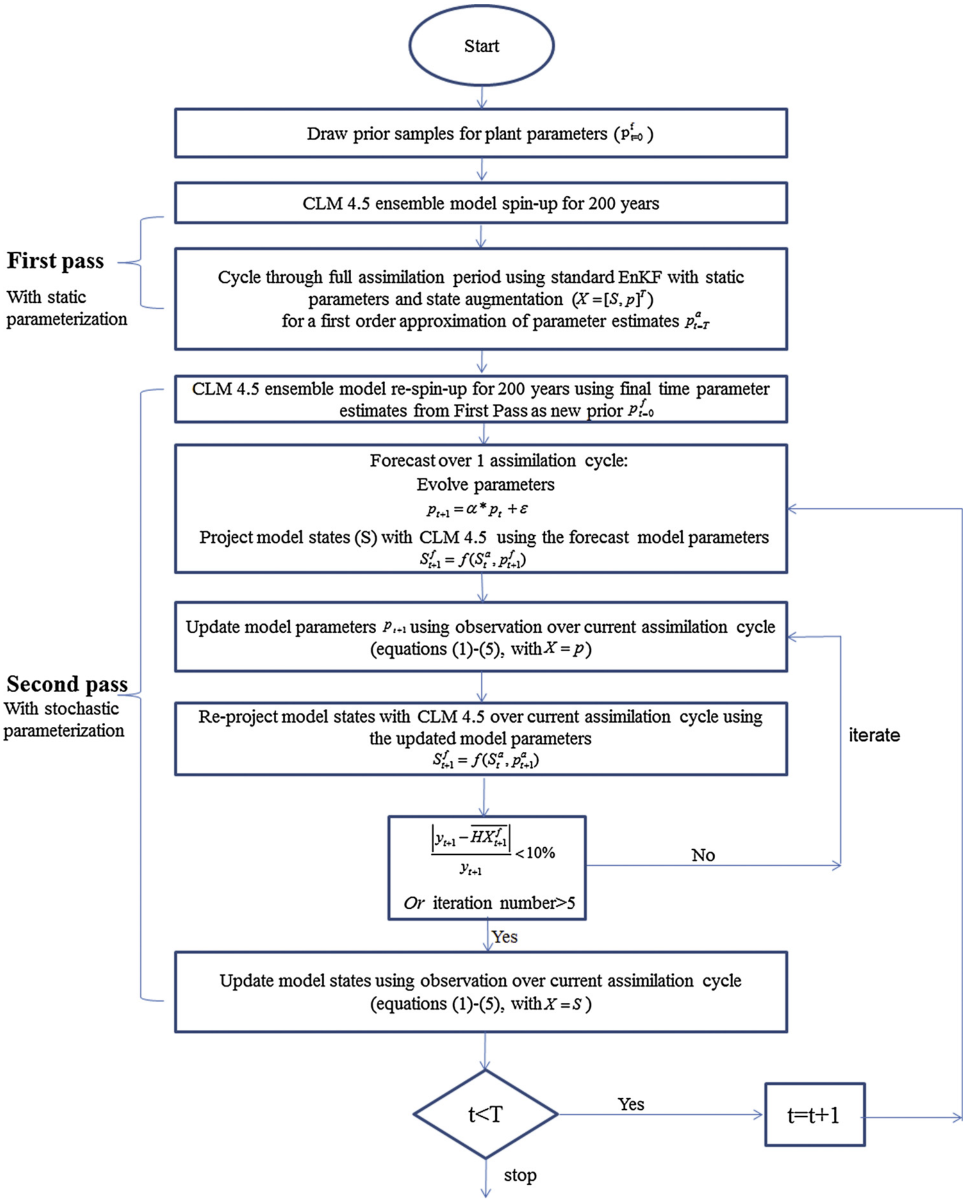

Fig. 2. Schematic of the two-tiered iterative EnKF implementation with stochastic parameterization. The function "f" represents forecast simulations with CLM 4.5; see text for other variable definitions. Note that for the static parameter comparison tests, a second pass is also implemented, but using the standard EnKF formulation from the first pass (no parameter evolution and no iteration of each assimilation cycle).

$$scMSE(t) = \frac{\frac{1}{b}\sum_{j=1}^{b}(\bar{\xi}^j(t) - \xi^j_{tr}(t))^2}{std(\xi^j)} for parameters$$
$$scMSE(t) = \frac{\frac{1}{b}\sum_{j=1}^{b}(\bar{\xi}^j(t) - \xi^j_{tr}(t))^2}{\xi^j_{tr}(t)} for states \tag{11}$$

In addition, the ratio of MSE to variance is examined for EnKF divergence (Sacher and Bartello, 2008), which occurs when the estimate fails to capture the true model values:

$$MSE: variance = \frac{MSE(t)}{\frac{1}{b}\sum_{j=1}^{b}Var(\xi^j)} \tag{12}$$

This ratio is ideally about 1 if the estimate uncertainty (variance) appropriately quantifies the estimate error (MSE). Consistently high values indicate over-confidence about a wrong estimate that EnKF may no longer be able to correct by assimilating observations, which can lead to filter divergence (Ng et al., 2011). A ratio less than 1 will not cause divergence, though it does convey more than necessary uncertainty about the estimate. Treating a temporally varying parameter as a static parameter – for example, in the standard EnKF implementation – could exacerbate problems of estimation divergence, because the parameter is not allowed to adequately vary. EnKF fixes such as variance inflation (Anderson and Anderson, 1999) and artificial parameter noise (Moradkhani et al., 2005) provide ad hoc solutions to divergence; a stochastic formulation could instead inject variability as a mechanistically consistent solution.

2.5. *Kelmet site setup*

After the synthetic tests, the data-conditioned stochastic parameterization approach is applied with in-situ soil moisture and MODIS LAI observations for Kelmet. As in the synthetic experiment, the input data, including the meteorological forcing and initial conditions, is from Kelmet. The main distinction from the synthetic experiment set-up is the simulation of the drought-deciduous-shrub PFT in addition to broadleaf-evergreen-shrub, in order to include co-dominant *Ambrosia*

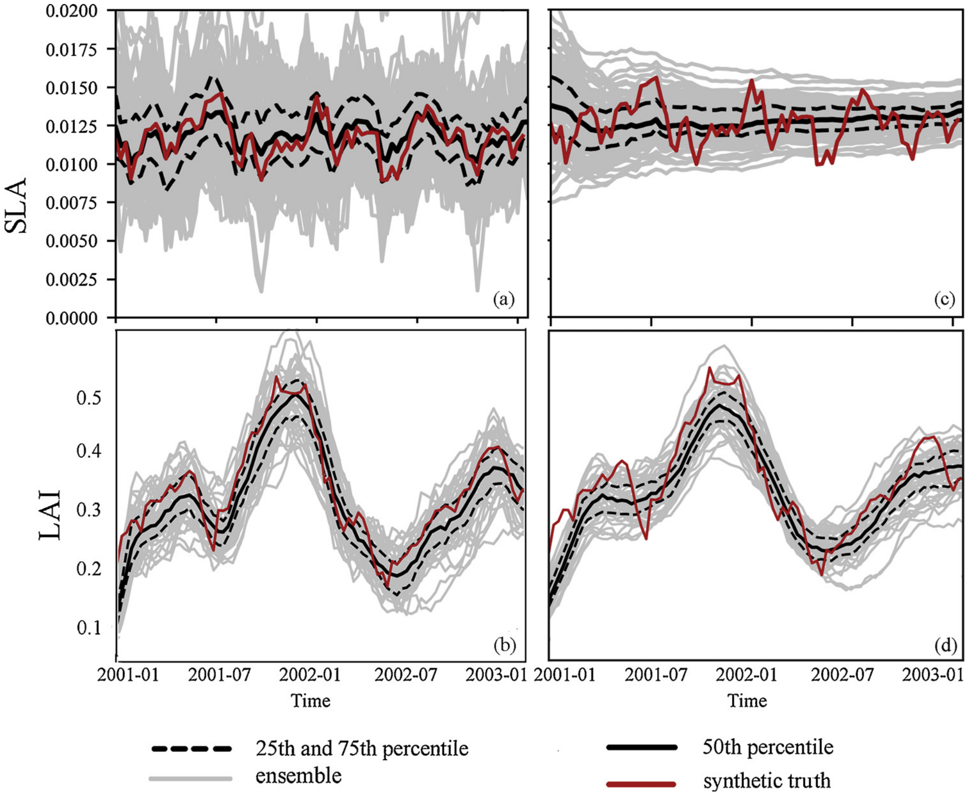

Fig. 3. Synthetic EnKF results using (a)-(b) stochastic parameterization and (c)-(d) static parameterization. Parameter estimates in (a) and (c) are results from the second pass in the two-tiered EnKF implementation. In the stochastic case, the second pass includes parameter perturbations, and posterior ensemble simulations of LAI in (b) use the full ensemble time series of conditioned SLA estimates in (a). In the static case, the second pass does not include parameter perturbations, and posterior ensemble simulations of LAI in (d) use the final time ensemble conditioned SLA estimates in (c).

dumosa alongside dominant *Larrea tridentata.* Separate model columns were implemented for the two plant types to represent complementary root distributions observed for the *Larrea tridentata-Ambrosia dumosa* shrub community (Wallace et al., 1980; Stevenson et al., 2009). The stochastic and static EnKF parameterization used with the Kelmet data is identical to the synthetic experiment. The results for the Kelmet site are plant parameters estimated for both broadleaf-evergreen-shrub and drought-deciduous-shrub types. The conditioned SLA time series is then compared against soil wetness to propose a stochastic model for predicting SLA plasticity based on environmental stressors. Finally, the ecohydrological implications of representing trait variability versus use of standard static parameters are explored.

3. Results

3.1. Synthetic experiment results

Results in Fig. 3(a) show that the stochastic parameterization successfully uncovers time-varying plant traits, with true time-varying SLA falling within the 25th to 50th percentile of the conditioned ensemble estimate. In comparison, the static parameterization converges to the time-average true SLA but fails to capture temporal patterns induced by water stress, with the ensemble estimate missing most of the high and low values (Fig. 3(c)). ScMSE and coefficient of variation results quantitatively confirm that the stochastic parameterization method outperforms the standard static method in estimating SLA temporal variation (Table 2). “Posterior simulations” in the stochastic case were generated by implementing the time series of data-conditioned parameters back into CLM 4.5. “Posterior simulations” in the standard static parameter case were generated using only the final time SLA estimate as a constant input. The stochastic approach generates LAI results that agree well with the synthetic true values (Fig. 3(b)). The static approach produces similar scMSE as the stochastic case, but the ensemble LAI trajectory exhibits too little dynamic variability and ensemble spread. In particular, for the static case, the truth often deviates outside the 25th-50th percentile estimate (Fig. 3(d)), the coefficient of variation of the estimate is lower than for the synthetic true case, and MSE:var ratio is greater than 1 (Table 2).

3.2. Kelmet site results

3.2.1. Data-conditioned stochastic shrub parameters

With in-situ soil moisture and MODIS LAI observations at the study site, the conditioned stochastic estimate of SLA shows clear temporal dynamics for the broadleaf-evergreen-shrub *Larrea tridentata* in Fig. 4(a) (coefficient of variation of 0.25). All trait estimates were constrained by the data-conditioning (Fig. S2), but none of the others showed discernible temporal variability (Fig. S3), including SLA for the broadleaf-deciduous-shrub *Ambrosia dumosa* (coefficient of variation of 0.07, see Fig. S4). This difference in temporal SLA patterns between the two shrub types would not have appeared with the standard static parameter EnKF, which also produced SLA estimates with minimal

Table 2
Summary of statistical results for SLA parameters and LAI using static and stochastic parameterizations. Reported errors for scMSE and MSE:variance are standard deviations of these metrics over time.

	scMSE		MSE:variance		Coefficient of Variation		
	Static	Stochastic	Static	Stochastic	Static	Stochastic	Truth
SLA	2.2 ± 0.79	0.63 ± 0.21	1.12 ± 0.48	0.68 ± 0.49	0.05	0.25	0.29
LAI	0.78 ± 0.34	0.73 ± 0.39	1.34 ± 0.41	0.80 ± 0.28	0.23	0.32	0.35

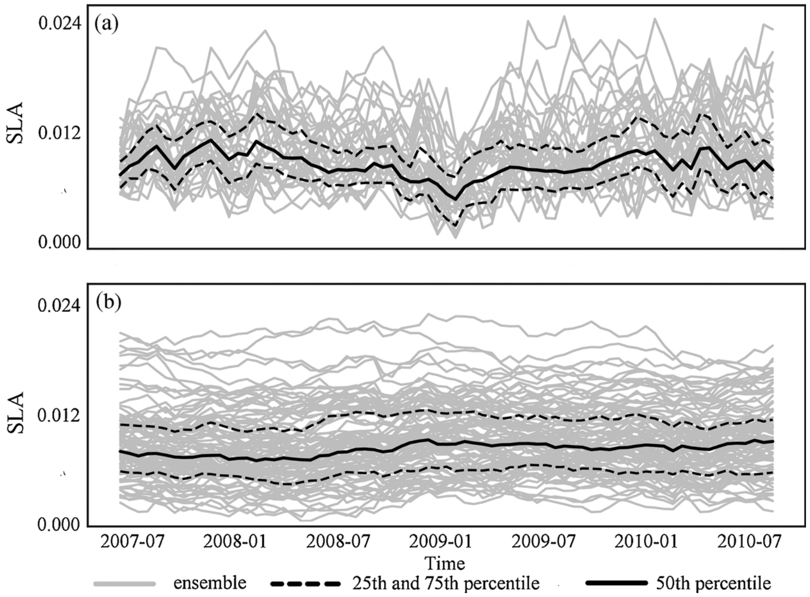

Fig. 4. Estimates of *Larrea tridentata* SLA from the second pass of the two-tiered EnKF implementation using (a) stochastic and (b) static parameterization. The second pass includes parameter perturbations for the stochastic case but not the static case.

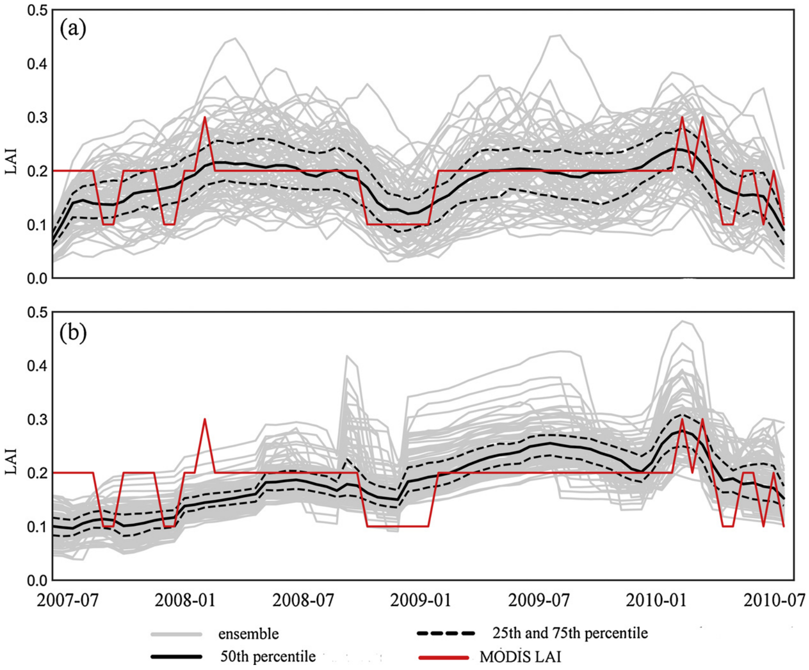

Fig. 5. Posterior simulated LAI using data-conditioned (a) stochastic and (b) static parameter estimates from Fig. 4. The MODIS LAI observational error is 0.1. The stochastic case (a) uses the full ensemble time series of conditioned SLA estimates from Fig. 4(a). The static case (b) uses the final time ensemble conditioned SLA estimates from Fig. 4(b).

variability for the broadleaf-evergreen-shrub PFT (Fig. 4(b)). For posterior LAI simulations (Fig. 5), the 25th to 75th percentile for both the static and stochastic case mostly correspond to MODIS values within observational error of 0.1, but the stochastic parameterization simulations track actual MODIS dynamics much more closely than the static parameterization. Compared to the stochastic results, the 25th to 75th percentile LAI results for the static case covers a narrower range that fails to encapsulate the MODIS observation during most of the period (Fig. 5(b)), demonstrating the importance of temporally variable SLA for simulating observed LAI dynamics.

3.2.2. *Hindcast with data-conditioned stochastic shrub parameters*

The stochastic SLA estimate for the broadleaf-evergreen-shrub PFT exhibits a statistically significant positive correlation with the 30-day averaged soil wetness factor (Fig. 6). This relationship not only presents water availability as a possible controlling factor on SLA trait variability, but it also enables stochastic trait predictions over time periods outside the observational period. To assess the potential ecohydrological importance of water stress-driven SLA variability over varying wet and dry periods, we statistically reconstructed monthly SLA over a 40-year historical interval (1960–2000) using a linear regression relationship based on the data-conditioned estimates. With two explanatory variables, SLA at the previous 30-day time step ($SLA(t-1)$) and the soil wetness factor averaged over the preceding 30 days, the regression model adequately reproduced the conditioned SLA over the observational period with a coefficient of determination (R^2) of 0.89 (Fig. S5).

Fig. 7a shows that ensemble hindcast simulations using the stochastically reconstructed SLA generates similar time-average results as simulations with static SLA, but the former generates monthly LAI with

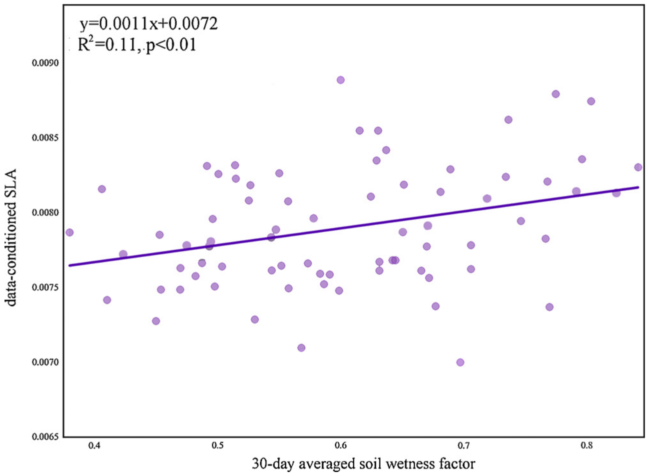

Fig. 6. Correlation between 30-day averaged soil wetness factor and data-conditioned SLA using stochastic parameterization.

greater seasonal variability due to dynamic SLA response to drought and wet events (Fig. S6). More variable LAI with stochastic SLA leads to transpiration simulations that are at times lower and at times higher than with static SLA (Fig. 7b), but importantly, stochastic SLA produces 31% greater cumulative gross primary productivity (GPP) (Fig. 7c) and on average 22% higher water use efficiency (WUE, defined as the ratio of GPP to transpiration) (Fig. 7d) over the 40-year period.

4. Discussion

4.1. Identifying SLA temporal variability

Here, we introduced a new data-model integration approach that utilizes globally available data to identify under-studied temporal variability of plant traits and generate stochastic-in-time model parameterizations. A synthetic test demonstrated that the new framework can successfully and robustly constrain time-varying trait values. Implementation with observations at the desert study site revealed temporal dynamics in the SLA trait for the common broadleaf-evergreen-shrub *Larrea tridentata* (Fig. 4). This includes variations of about 25% over the 3.5 years observational period, over values that are close to previous field measurements (0.008 $m^2 g^{-1}C$, Chew and Chew, 1965).

SLA temporal variability has not been previously examined in desert shrubs to our knowledge, but observations on seasonal (Damesin et al., 1998; Damesin and Lelarge, 2003; Reich et al., 1997; Wilson et al., 2000; Xu and Baldocchi, 2003; Grassi et al., 2005; Misson et al., 2006; Nouvellon et al., 2010) and interannual time scales (Dawson and Bliss, 1993; Abrams, 1994; Ma et al., 2011) in other ecosystems support the possibility of temporal SLA variability found with our new stochastic framework for *Larrea tridentata*. The few temporal SLA studies on evergreen plants (not in deserts) show ranges of variability that are similar to our results. For example, Nouvellon et al (2010) showed that the stand-average SLA in a clonal *Eucalyptus* varied by about 20% within one year, and Misson et al. (2006) reported a similar magnitude change of 28% between seasons for *Pinus ponderosa* in the Sierra Nevada mountains of California. Seasonal changes of SLA in deciduous species are often thought to be larger than in evergreen species (Wilson et al., 2000; Xu and Baldocchi, 2003; Grassi et al., 2005), which is counter to the lack of temporal variability detected for the drought-deciduous-shrub PFT in our study. It is possible that because co-dominant *Ambrosia dumosa* covers only a third of the ground area as dominant *Larrea tridentata* at the study site, 1-km MODIS LAI is too coarse to detect its SLA variability and/or distinguish its effect from the drought-deciduous phenology (see Oleson et al., (2013) for details on CLM 4.5′s phenology scheme).

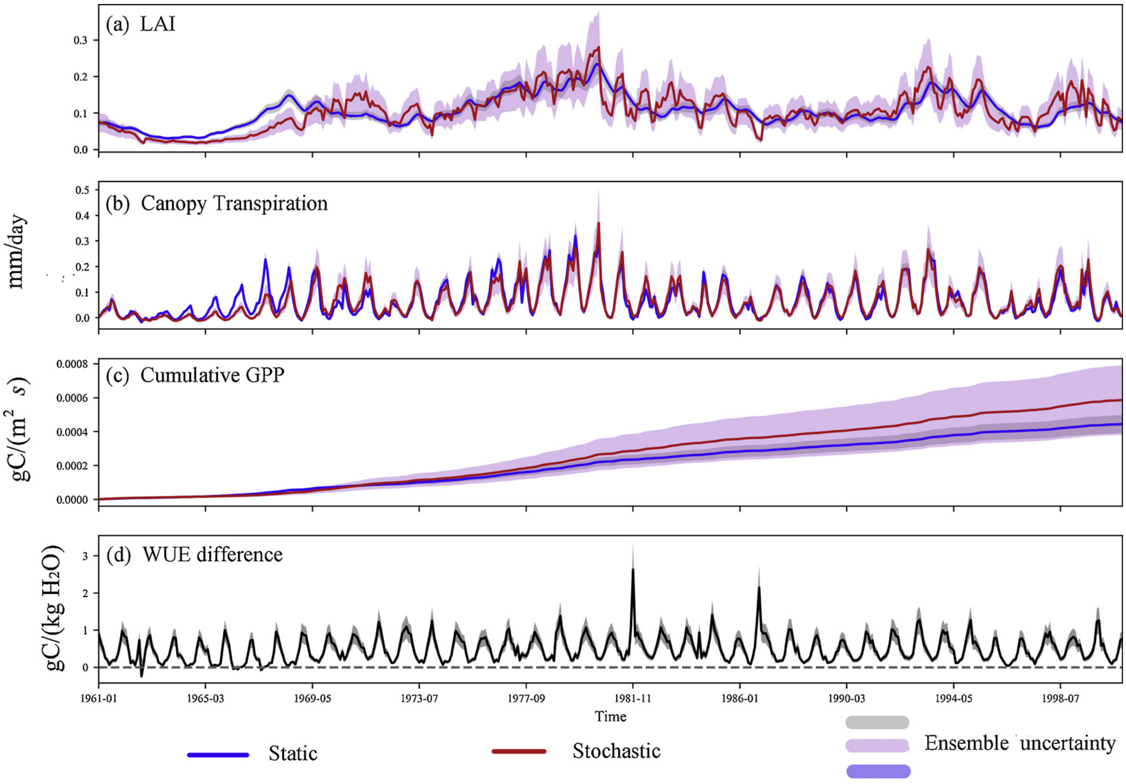

Fig. 7. Comparison of hindcast simulations of (a) LAI, (b) canopy transpiration, (c) cumulative GPP, and (d) water use efficiency (WUE) difference (defined as stochastic minus static) for the stochastic and static parameterizations.

4.2. Temporal variability of other traits

The lack of discernible temporal variability in traits other than SLA was unexpected. Generally, change in one trait compensates changes in other traits because of resource allocation among plant organs (Kleyer and Minden, 2015); this serves as the underlying mechanism for the economic spectrum of leaves. For example, species with a shorter leaf lifespan usually have lower leaf nitrogen per area and higher SLA and can exhibit greater net photosynthetic rates (Reich et al., 1997; Wright et al., 2004; Kikuzawa and Lechowicz, 2006). Compared with well-documented leaf traits, the connection between roots traits and whole-plant structure and function is less well-understood (McCormack et al., 2017) due to harder-to-observe links and a lack of standardized sampling protocols for roots. Seasonality of fine-root traits has become increasingly recognized (Zadworny et al., 2015; Pregitzer et al., 1998; Volder et al., 2005), although how these correlate with other plant traits remains uncertain.

Although other trait estimates have much lower temporal variability (coefficients of variation of < 0.05) than SLA for *Larrea tridentata* (coefficient of variation of 0.2), leaf longevity estimates do have expected negative ensemble correlations with SLA and positive correlations with leaf nitrogen per area (Na) that are statistically significant ($p < 0.01$) (Figure S7), but these correlations are weak. We do note that leaf trait relationships derived from the TRY database show a similar magnitude of correlation coefficient between SLA and leaf N per area (absolute value of correlation coefficient = 0.39, left side of Fig. S8) to that found between our estimated SLA and other parameters (absolute values of correlation coefficients less than or approximately 0.3, Fig. S7). It is possible that our slightly weaker correlations could be because the seasonal time scale over which SLA is found to vary is insufficient for plants to fully adjust physiologically. Because trait covariation studies typically rely on spatial data (*e.g.* Reich et al., 2018), the amount of time needed at a specific location for plant functional trade-offs to develop is not well-explored. Another possibility for the weak trait correlations is that LAI and soil moisture data may be inadequate for constraining other traits that may in fact co-vary strongly with SLA over the observational period. Sensitivity tests with CLM show that the variability of leafcn (the ratio of carbon to nitrogen in leaves), for example, has negligible effect on LAI and soil moisture predictions (Fig. S8). This indicates that other relevant observations – such as leaf nitrogen, root chemistry, and/or longer-term records – could be necessary to reveal potential plasticity of other trait parameters in CLM 4.5, such as carbon to nitrogen ratios, root distribution, and leaf longevity.

4.3. Environmental stress-driven SLA plasticity

The statistically significant correlation found between the stochastic SLA estimate for *Larrea tridentata* and seasonal water availability (Fig. 6) presents the case for environmental stress-driven trait plasticity in evergreen desert shrubs, which we represented with a temporally stochastic regression model for SLA based on soil wetness. Corroborating our findings in a different but also moisture-limited ecosystem, Gratani and Varone (2006) measured morphological and phenological traits of multiple evergreen shrub types (*Rosmarinus officinalis L*, *Erica multiflora L*, *Erica arborea L*) in a semi-arid Mediterranean region and showed that interannually, SLA decreased in response to decreased rainfall. A temporal relationship between SLA and water availability has also been reported for evergreen species in other ecosystems, such as *E. tetrondonta* (Prior et al., 2004), *E. globulus* (Faria et al., 2008), *Pinus ponderosa* (Misson et al., 2006), and *Eucalyptus* (Warren et al., 2006; Nouvellon et al., 2010).

In addition to leaf-level plasticity, water availability may also indirectly affect plot-level SLA at our site by modifying leaf demographics, because SLA of older leaves is generally lower than SLA of younger leaves (England and Attiwill, 2008; Laclau et al., 2009). Adequate moisture conditions can influence the ratio of young to older biomass by promoting leaf production and slowing leaf shedding (Pook, 1984). Leaf demography is not explicitly represented in CLM 4.5, although there have been recent efforts to incorporate it (Fisher et al., 2015).

Our results show how data-conditioned stochastic parameter estimates can reveal possible trait plasticity in time that has not yet been explored. Importantly, such model-based discoveries of potential plasticity can motivate and direct more laborious and costly repeat field campaigns to investigate actual physiological shifts and mechanisms. We envision future iterations of our method will use such observations to further condition stochastic parameterizations, as well as new hyperspectral and spectro-radiometric data types that are proving effective for tracking plant traits over time (Serbin et al., 2014; Yang et al., 2016).

4.4. Ecohydrological implications of SLA plasticity

Our model results show temporally variable SLA to be necessary for simulating observed LAI dynamics (Figs. 3 and 5). Because of LAI's role in scaling leaf physiological functions such as transpiration and photosynthesis to the canopy level and beyond, we would then expect the inferred SLA plasticity to strongly impact ecohydrological fluxes. The 40-year hindcast simulation using stochastic SLA – reconstructed with the regression-based plasticity model – served to test this. Results indicate that temporal SLA variability at the study site not only marks a response to environmental conditions, but it also appears to act as an adaptation that aids in ecological function – including GPP and WUE (Fig. 7). SLA plasticity has been previously proposed as a way for plants to increase the efficiency of light-harvesting and/or resource-use under varying light, atmospheric deposition, nutrient status, and water availability (Poorter et al., 2009). Specifically with water limitation, plant growth slows and can exhibit lower SLA with tighter-packed photosynthetically active tissue, which allows for more efficient water-use through a relatively smaller surface. Our work provides the first ecohydrological modeling effort to our knowledge to incorporate moisture stress-driven SLA plasticity, for which detailed physiological regulation remains unclear (Poorter et al., 2009). Previous modeling studies for forest management have attempted to empirically describe SLA as dependent on nitrogen supply (Battaglia et al., 2004; Corbeels et al., 2005) and stand age (Sands and Landsberg, 2002; Almeida et al., 2004; Fontes et al., 2006) but do not readily extend to other ecosystems under different environmental controls.

Temporal SLA trait variability has not been previously studied in desert shrubs to our knowledge, but our model-based results suggest that environmental stress-driven plasticity – on an individual leaf, plant, or plot-level – could play a key role in maintaining favorable productivity and resource efficiency through highly variable and unreliable moisture conditions. Our work highlights the need for incorporating SLA and other trait plasticity into models. We showed that the standard static parameter approach failed to capture plant responses to environmental change, and that its narrower representation of uncertainty (compared to the stochastic approach) can lead to biased predictions that diverge from actual dynamic conditions. We anticipate that implementing our stochastic-in-time approach across ecosystems can extend our understanding about trait variability beyond sparse plant trait databases (*e.g.*, TRY) and improve our ability to simulate carbon and water fluxes in response to global change.

Author contributions

SL, GCN designed and performed the research; SL and GCN wrote the paper.

Acknowledgement

This study was supported by funding from NSF (NSF-1724781). Supercomputing resources were provided by the Minnesota Supercomputing Institute (MSI) at University of Minnesota-Twin Cities and the Cheyenne cluster at NCAR. The authors thank Peter Reich (University of Minnesota) for valuable conversations about the TRY database and trait variability at the inception of the project; Ethan Butler (University of Minnesota) also provided insightful suggestions about model interpretations. Two anonymous reviewers contributed comments that helped with the clarity of this paper. This study utilized data from the TRY initiative on plant traits (http://www.try-db.org). The TRY initiative and database is hosted, developed and maintained by J. Kattge and G. Bönisch (Max Planck Institute for Biogeochemistry, Jena, Germany).

Appendix A. Supplementary data

Supplementary material related to this article can be found, in the online version, at doi:https://doi.org/10.1016/j.agrformet.2019.05.005.

References

Abrams, M.D., 1994. Genotypic and phenotypic variation as stress adaptations in temperate tree species: a review of several case studies. Tree Physiol. 14, 833–842.

Ainsworth, E.A., Rogers, A., 2007. The response of photosynthesis and stomatal conductance to rising CO_2: mechanisms and environmental interactions. Plant Cell Environ. 30, 258–270.

Almeida, A.C., Landsberg, J.J., Sands, P.J., 2004. Parameterisation of 3-PG model for fast-growing *Eucalyptus* grandis plantations. For. Ecol. Manage. 193, 179–195.

Anderson, J.L., Anderson, S.L., 1999. A monte carlo implementation of the nonlinear filtering problem to produce ensemble assimilations and forecasts. Mon. Weather. Rev. 127, 2741–2758.

Atkin, O.K., Tjoelker, M.G., 2003. Thermal acclimation and the dynamic response of plant respiration to temperature. Trends Plant Sci. 8, 343–351.

Atkin, O.K., Edwards, E.J., Loveys, B.R., 2000. Response of root respiration to changes in temperature and its relevance to global warming. New Phytol. 147, 141–154.

Barbour, M.G., 1969. Age and space distribution of the desert shrub *Larrea div aricata*. Ecology 50, 679–685.

Battaglia, M., Sands, P., White, D., Mummery, D., 2004. CABALA: a linked carbon, water and nitrogen model of forest growth for silvicultural decision support. For. Ecol. Manage. 193, 251–282.

Bedford, D.R., Miller, D.M., Schmidt, K.M., Phelps, G.A., et al., 2009. Landscape-scale relationships between surficial geology, soil texture, topography, and creosote bush size and density in the Eastern Mojave Desert of California. In: Webb, R.H. (Ed.), The Mojave Desert: Ecosystem Processes and Sustainability. Univ. of Nevada Press, Reno, pp. 252–277.

Butler, E.E., Datta, A., Flores-Moreno, H., et al., 2017. Mapping local and global variability in plant trait distributions. Proceedings of the National Academy of Sciences.

Chew, R.M., Chew, A.E., 1965. The primary productivity of a desert-shrub (*Larrea tridentata*) community. Ecol. Monogr. 35, 355–375.

Christensen, H.M., Moroz, I.M., Palmer, T.N., 2015. Stochastic and perturbed parameter representations of model uncertainty in convection parameterization. J. Atmos. Sci. 72, 2525–2544.

Corbeels, M., McMurtrie, R.E., Pepper, D.A., Mendham, D.S., Grove, T.S., O'Connell, A.M., 2005. Long-term changes in productivity of *Eucalypt* plantations under different harvest residue and nitrogen management practices: a modelling analysis. For. Ecol. Manage. 217, 1–18.

Coyle, J.R., Halliday, F.W., Lopez, B.E., Palmquist, K.A., Wilfahrt, P.A., Hurlbert, A.H., 2014. Using trait and phylogenetic diversity to evaluate the generality of the stress-dominance hypothesis in eastern North American tree communities. Ecography 37, 814–826.

Dagan, G., 1986. Statistical theory of groundwater flow and transport: pore to laboratory, laboratory to formation, and formation to regional scale. Water Resour. Res. 22, 120S–134S.

Damesin, C., Lelarge, C., 2003. Carbon isotope composition of current-year shoots from *Fagus sylvatica* in relation to growth, respiration and use of reserves. Plant Cell Environ. 26, 207–219.

Damesin, C., Rambal, S., Joffre, R., 1998. Co-occurrence of trees with different leaf habit: a functional approach on Mediterranean oaks. Acta Oecologica 19, 195–204.

Dawson, T.E., Bliss, L.C., 1993. Plants as mosaics: leaf-, ramet-, and gender-level variation in the physiology of the *dwarf willow, Salix arctica*. Funct. Ecol. 7, 293–304.

Eagleson, P.S., 1978. Climate, soil, and vegetation: 1. Introduction to water balance dynamics. Water Resour. Res. 14, 705–712.

England, J.R., Attiwill, P.M., 2008. Patterns of growth and nutrient accumulation in expanding leaves of *Eucalyptus regnans* (Myrtaceae). Aust. J. Bot. 56, 44–50.

Evensen, G., 1994. Sequential data assimilation with a nonlinear quasi-geostrophic model using Monte Carlo methods to forecast error statistics. J. Geophys. Res. Oceans 99, 10143–10162.

Evensen, G., 2009. The ensemble Kalman filter for combined state and parameter estimation. Ieee Control. Syst. Mag. 29, 83–104.

Faria, T., Silvério, D., Breia, E., et al., 2008. Differences in the response of carbon assimilation to summer stress (water deficits, high light and temperature) in four Mediterranean tree species. Physiol. Plant. 102, 419–428.

Fisher, R.A., Muszala, S., Verteinstein, M., et al., 2015. Taking off the training wheels: the properties of a dynamic vegetation model without climate envelopes, CLM4.5(ED). Geosci. Model. Dev. 8, 3593–3619.

Fontes, L., Landsberg, J., Tomé, J., Tomé, M., Pacheco, C.A., Soares, P., Araujo, C., 2006. Calibration and testing of a generalized process-based model for use in Portuguese *Eucalyptus* plantations. Can. J. For. Res. 36, 3209–3221.

Gelhar, L.W., 1986. Stochastic subsurface hydrology from theory to applications. Water Resour. Res. 22, 135S–145S.

Grassi, G., Vicinelli, E., Ponti, F., Cantoni, L., Magnani, F., 2005. Seasonal and interannual variability of photosynthetic capacity in relation to leaf nitrogen in a deciduous forest plantation in northern Italy. Tree Physiol. 25, 349–360.

Gratani, L., Varone, L., 2006. Long-time variations in leaf mass and area of Mediterranean evergreen broad-leaf and narrow-leaf maquis species. Photosynthetica 44, 161–168.

Gu, Y., Oliver, D.S., 2007. An iterative ensemble kalman filter for multiphase fluid flow data assimilation. Spe J. 12, 438–446.

Hansen, J.A., Penland, C., 2007. On stochastic parameter estimation using data assimilation. Physica D 230, 88–98.

Hendricks Franssen, H.J., Kinzelbach, W., 2008. Real-time groundwater flow modeling with the Ensemble Kalman Filter: joint estimation of states and parameters and the filter inbreeding problem. Water Resour. Res. 44, 1–21.

Juricke, S., Lemke, P., Timmermann, R., Rackow, T., 2012. Effects of stochastic ice strength perturbation on Arctic finite element sea ice modeling. J. Clim. 26, 3785–3802.

Kattge, J., Díaz, S., Lavorel, S., et al., 2011. TRY - a global database of plant traits. Glob. Chang. Biol. 17, 2905–2935.

Kikuzawa, K., Lechowicz, M.J., 2006. Toward synthesis of relationships among leaf longevity, instantaneous photosynthetic rate, lifetime leaf carbon gain, and the gross primary production of forests. Am. Nat. 168, 373–383.

Kitsios, V., Frederiksen, J.S., Zidikheri, M.J., 2014. Scaling laws for parametrizations of subgrid interactions in simulations of oceanic circulations. Philosophical Transactions of the Royal Society A: mathematical. Phys. Eng. Sci. 372.

Kleyer, M., Minden, V., 2015. Why functional ecology should consider all plant organs: An allocation-based perspective. Basic Appl. Ecol. 16, 1–9.

Laclau, J.-P., Almeida, J.C.R., Gonçalves, J.L.M., et al., 2009.) Influence of nitrogen and potassium fertilization on leaf lifespan and allocation of above-ground growth in *Eucalyptus* plantations. Tree Physiol. 29, 111–124.

Leakey, A.D.B., Ainsworth, E.A., Bernacchi, C.J., Rogers, A., Long, S.P., Ort, D.R., 2009. Elevated CO_2 effects on plant carbon, nitrogen, and water relations: six important lessons from FACE. J. Exp. Bot. 60, 2859–2876.

Ma, S., Baldocchi, D.D., Mambelli, S., Dawson, T.E., 2011. Are temporal variations of leaf traits responsible for seasonal and inter-annual variability in ecosystem CO_2 exchange? Funct. Ecol. 25, 258–270.

Mccormack, M.L., Guo, D., Iversen, C.M., et al., 2017. Building a better foundation: improving root-trait measurements to understand and model plant and ecosystem processes. New Phytol. 27–37.

Miller, D.M., Bedford, D.R., Hughson, D.L., McDonald, E.V., Robinson, S.E., Schmidt, K.M., et al., 2009. Mapping mojave desert ecosystem properties with surficial geology. In: Webb, R.H. (Ed.), The Mojave Desert: Ecosystem Processes and Sustainability. Univ. of Nevada Press, Reno, pp. 225–251.

Mirus, B.B., Perkins, K.S., Nimmo, J.R., Singha, K., 2009. Hydrologic Characterization of Desert Soils with Varying Degrees of Pedogenesis: 2. Inverse Modeling for Effective Properties. Vadose Zone J. 8, 496–509.

Misson, L., Tu, K.P., Boniello, R.A., Goldstein, A.H., 2006. Seasonality of photosynthetic parameters in a multi-specific and vertically complex forest ecosystem in the Sierra Nevada of California. Tree Physiol. 26, 729–741.

Moradkhani, H., Sorooshian, S., Gupta, H.V., Houser, P.R., 2005. Dual state-parameter estimation of hydrological models using ensemble Kalman filter. Adv. Water Resour. 28, 135–147.

Muraoka, H., Saigusa, N., Nasahara, K.N., et al., 2010. Effects of seasonal and interannual variations in leaf photosynthesis and canopy leaf area index on gross primary production of a cool-temperate deciduous broadleaf forest in Takayama. Japan. J. Plant Res. 123, 563–576.

Ng, G.H.C., Mclaughlin, D., Entekhabi, D., Ahanin, A., 2011. The role of model dynamics in ensemble Kalman filter performance for chaotic systems. Tellus A 63, 958–977.

Ng, G.H.C., Bedford, D., Miller, D., 2014. A mechanistic modeling and data assimilation framework for Mojave Desert ecohydrology. Water Resour. Res. 4662–4685.

Ng, G.H.C., Bedford, D.R., Miller, D.M., 2015. Identifying multiple time scale rainfall controls on Mojave Desert ecohydrology using an integrated data and modeling approach for *Larrea tridentata*. Water Resour. Res. 51, 3884–3899.

Nicotra, A.B., Atkin, O.K., Bonser, S.P., et al., 2010. Plant phenotypic plasticity in a changing climate. Trends Plant Sci. 15, 684–692.

Nimmo, J.R., Perkins, K.S., Schmidt, K.M., Miller, D.M., Stock, J.D., Singha, K., 2009. Hydrologic characterization of desert soils with varying degrees of pedogenesis: 1. field experiments evaluating plant-relevant soil water behavior. Vadose Zone J. 8, 480–495.

Nouvellon, Y., Laclau, J.P., Epron, D., et al., 2010. Within-stand and seasonal variations of specific leaf area in a clonal *Eucalyptus* plantation in the Republic of Congo. For. Ecol. Manage. 259, 1796–1807.

Oleson, K.W., Lawrence, D.M., B G, et al., 2013. Technical Description of Version 4.5 of the Community Land Model (CLM).

Ordoñez, J.C., Van Bodegom, P.M., J-PM, Witte, Wright, I.J., Reich, P.B., Aerts, R., 2009. A global study of relationships between leaf traits, climate and soil measures of nutrient fertility. Glob. Ecol. Biogeogr. 18, 137–149.

Palmer, T.N., 2012. Towards the probabilistic Earth-system simulator: a vision for the future of climate and weather prediction. Q. J. R. Meteorol. Soc. 138, 841–861.

Palmer, T.N., Buizza, R., Doblas-Reyes, F., et al., 2009. Stochastic parametrization and model uncertainty. ECMWF Technical Memorandum 598.

Pappas, C., Fatichi, S., Burlando, P., 2016. Modeling terrestrial carbon and water dynamics across climatic gradients: does plant trait diversity matter? New Phytol. 209, 137–151.

Pavlick, R., Drewry, D.T., Bohn, K., Reu, B., Kleidon, A., 2012. The jena diversity-dynamic global vegetation model (JeDi-DGVM): a diverse approach to representing terrestrial biogeography and biogeochemistry based on plant functional trade-offs. Biogeosciences Discuss. 9, 4627–4726.

Pook, E.W., 1984. Canopy dynamics of Eucalyptus maculata hook. I. Distribution and dynamics of leaf populations. Aust. J. Bot. 32, 387–403.

Poorter, H., Niinemets, Ü, Poorter, L., et al., 2009. Causes and consequences of variation in leaf mass per area (LMA): a meta-analysis. New Phytol. 182, 565–588.

Pregitzer, K.S., Laskowski, M.J., Burton, A.J., Lessard, V.C., Zak, D.R., 1998. Variation in sugar maple root respiration with root diameter and soil depth. Tree Physiol. 18, 665–670.

Prior, L.D., DMJS, Bowman, Eamus, D., 2004. Seasonal differences in leaf attributes in Australian tropical tree species: family and habitat comparisons. Funct. Ecol. 18, 707–718.

Reich, P.B., Walters, M.B., Ellsworth, D.S., 1997. From tropics to tundra: global convergence in plant functioning. Proceedings of the National Academy of Sciences. 94, 13730 LP-13734.

Reich, P.B., Walters, M.B., Ellsworth, D.S., 2018. Leaf age and season influence the relationships between leaf nitrogen, leaf mass per area and photosynthesis in maple and oak trees. Plant Cell Environ. 14, 251–259.

Ricciuto, D., Sargsyan, K., Thornton, P., 2017. The Impact of Parametric Uncertainties on Biogeochemistry in the E3SM Land Model. J. Adv. Model. Earth Syst. 10, 297–319.

Rodriguez-Iturbe, I., Porporato, A., Laio, F., Ridolfi, L., 2001. Plants in water-controlled ecosystems: active role in hydrologic processes and response to water stress: I. Scope and general outline. Adv. Water Resour. 24, 695–705.

Rundel, P.W., Gibson, A.C., 2005. Ecological Communities and Processes in a Mojave Desert Ecosystem. Cambridge Univ. Press, N. Y.

Ryu, Y., Baldocchi, D.D., Kobayashi, H., et al., 2011. Integration of MODIS land and atmosphere products with a coupled-process model to estimate gross primary productivity and evapotranspiration from 1 km to global scales. Global Biogeochem. Cycles 25 n/a-n/a.

Sacher, W., Bartello, P., 2008. Sampling Errors in Ensemble Kalman Filtering. Part I: Theory. Mon. Weather. Rev. 136, 3035–3049.

Sakov, P., Oliver, D.S., Bertino, L., 2012. An Iterative EnKF for Strongly Nonlinear Systems. Mon. Weather. Rev. 140, 1988–2004.

Sands, P.J., Landsberg, J.J., 2002. Parameterisation of 3-PG for plantation grown *Eucalyptus* globulus. For. Ecol. Manage. 163, 273–292.

Sato, H., Itoh, A., Kohyama, T., 2007. SEIB–DGVM: a new dynamic global vegetation Model using a spatially explicit individual-based approach. Ecol. Modell. 200, 279–307.

Schwinning, S., Sandquist, D.R., Miller, D.M., Bedford, D.R., Phillips, S.L., Belnap, J., 2011. The influence of stream channels on distributions of *Larrea tridentata* and *Ambrosia dumosa* in the Mojave Desert, CA, USA: patterns, mechanisms and effects of stream redistribution. Ecohydrology 4, 12–25.

Serbin, S.P., Singh, A., McNeil, B.E., Kingdon, C.C., Townsend, P.A., 2014. Spectroscopic determination of leaf morphological and biochemical traits for northern temperate and boreal tree species. Ecol. Appl. 24, 1651–1669.

Shen, W., Jenerette, G.D., Hui, D., Phillips, R.P., Ren, H., 2008. Effects of changing precipitation regimes on dryland soil respiration and C pool dynamics at rainfall event, seasonal and interannual scales. J. Geophys. Res. Biogeosci. 113.

Stevenson, B.A., McDonald, E.V., Caldwell, T.G., et al., 2009. Root patterns for *larrea tridentata* in relation to soil morphology in mojave desert soils of different ages geology. In: Webb, R.H. (Ed.), The Mojave Desert: Ecosystem Processes and Sustainability. Univ. of Nevada Press, Reno, pp. 312–338.

Strain, B.R., Chase, V.C., 1966. Effect of past and prevailing temperatures on the carbon dioxide exchange capacities of some woody desert perennials. Ecology 47, 1043–1045.

Uriarte, M., Canham, C.D., Thompson, J., et al., 2009. Natural disturbance and human land use as determinants of tropical forest dynamics: results from a forest simulator. Ecol. Monogr. 79, 423–443.

Van Kleunen, M., Fischer, M., 2007. Progress in the detection of costs of phenotypic plasticity in plants. New Phytol. 176, 727–730.

Verheijen, L.M., Brovkin, V., Aerts, R., et al., 2013. Impacts of trait variation through observed trait–climate relationships on performance of an Earth system model: a conceptual analysis. Biogeosciences 10, 5497–5515.

Verheijen, L.M., Aerts, R., Brovkin, V., Cavender-Bares, J., Cornelissen, J.H.C., Kattge, J., van Bodegom, P.M., 2015. Inclusion of ecologically based trait variation in plant functional types reduces the projected land carbon sink in an earth system model. Glob. Chang. Biol. 21, 3074–3086.

Villar, R., Marañón, T., Quero, J.L., Panadero, P., Arenas, F., Lambers, H., 2005. Variation in relative growth rate of 20 *Aegilops* species (Poaceae) in the field: the importance of net assimilation rate or specific leaf area depends on the time scale. Plant Soil 272, 11–27.

Vitasse, Y., Bresson, C.C., Kremer, A., Michalet, R., Delzon, S., 2010. Quantifying phenological plasticity to temperature in two temperate tree species. Funct. Ecol. 24, 1211–1218.

Volder, A., Smart, D.R., Bloom, A.J., Eissenstat, D.M., 2005. Rapid decline in nitrate uptake and respiration with age in fine lateral roots of grape: implications for root efficiency and competitive effectiveness. New Phytol. 165, 493–502.

Wallace, A., Romney, E.M., Cha, J.W., 1980. Depth distribution of roots of some perennial plants in the nevada test site area of the northern Mojave Desert. Gt. Basin Nat. Mem. 201–207.

Wang, Y.P., Lu, X.J., Wright, I.J., Dai, Y.J., Rayner, P.J., Reich, P.B., 2012. Correlations among leaf traits provide a significant constraint on the estimate of global gross primary production. Geophys. Res. Lett. 39, 1–7.

Warren, C.R., Dreyer, E., Tausz, M., Adams, M.A., 2006. Ecotype adaptation and acclimation of leaf traits to rainfall in 29 species of 16-year-old *Eucalyptus* at two common gardens. Funct. Ecol. 20, 929–940.

Westoby, M., Falster, D.S., Moles, A.T., Vesk, P.A., Wright, I.J., 2002. Plant ecological strategies: some leading dimensions of variation between species. Annu. Rev. Ecol. Syst. 33, 125–159.

Whitaker, J.S., Hamill, T.M., 2002. Ensemble data assimilation without perturbed observations. Mon. Weather. Rev. 130, 1913–1924.

White, M.A., Thornton, P.E., Running, S.W., Nemani, R.R., 2000. Parameterization and sensitivity analysis of the BIOME-BGC terrestrial ecosystem model: net primary production controls. Earth Interact. 4, 1–85.

Wilson, K.B., Baldocchi, D.D., Hanson, P.J., 2000. Spatial and seasonal variability of photosynthetic parameters and their relationship to leaf nitrogen in a deciduous forest. Tree Physiol. 20, 565–578.

Wright, I.J., Reich, P.B., Westoby, M., 2001. Strategy shifts in leaf physiology, structure and nutrient content between species of high- and low-rainfall and high- and low-nutrient habitats. Funct. Ecol. 15, 423–434.

Wright, I.J., Reich, P.B., Westoby, M., et al., 2004. The worldwide leaf economics spectrum. Nature 428, 821.

Wright, I.J., Reich, P.B., Cornelissen, J.H.C., et al., 2005. Modulation of leaf economic traits and trait relationships by climate. Glob. Ecol. Biogeogr. 14, 411–421.

Xu, L., Baldocchi, D.D., 2003. Seasonal trends in photosynthetic parameters and stomatal conductance of blue oak (*Quercus douglasii*) under prolonged summer drought and high temperature. Tree Physiol. 23, 865–877.

Yang, X., Tang, J., Mustard, J.F., Wu, J., Zhao, K., Serbin, S., Lee, J.E., 2016. Seasonal variability of multiple leaf traits captured by leaf spectroscopy at two temperate deciduous forests. Remote Sens. Environ. 179, 1–12.

Zadworny, M., McCormack, M.L., Rawlik, K., Jagodziński, A.M., 2015. Seasonal variation in chemistry, but not morphology, in roots of *Quercus robur* growing in different soil types. Tree Physiol. 35, 644–652.